Role of individual and population heterogeneity in shaping dynamics of multi-pathogen shedding in an island endemic bat

Samantha Aguillon[1*], Magali Turpin[1], Gildas Le Minter[1], Camille Lebarbenchon[1], Axel O. G. Hoarau[1], Céline Toty[1], Avril Duchet[1], Léa Joffrin[1#], Riana V. Ramanantsalama[1$], Pablo Tortosa[1], Patrick Mavingui[1] & Muriel Dietrich[1*]

[1]UMR PIMIT (Processus Infectieux en Milieu Insulaire Tropical), Université de la Réunion / INSERM1187 / CNRS9192 / IRD249, 97490 Sainte-Clotilde, Reunion Island

[#]Current address: Evolutionary Ecology Group, Department of Biology, University of Antwerp, Universiteitsplein 1, 2610 Antwerp, Belgium

[$]Current address: Behavioral Ecology & Sociobiology Unit, German Primate Center, Kellnerweg 4, 37077 Göttingen, Germany

*Samantha Aguillon - UMR PIMIT, Sainte-Clotilde, Reunion Island.

Email: samantha.aguillon@univ-reunion.fr

*Muriel Dietrich - UMR PIMIT, Sainte-Clotilde, Reunion Island.

Email: muriel.dietrich@ird.fr

Author Contributions:

Samantha Aguillon: Conceptualization (equal); formal analysis (lead); investigation (equal); visualization (lead); writing – original draft (lead); writing – review and editing (equal). Magali Turpin: Investigation (equal); writing – review and editing (equal); Gildas Le Minter: Investigation (equal); writing – review and editing (equal). Camille Lebarbenchon: Investigation (equal); writing – review and editing (equal). Axel O. G. Hoarau: Investigation (equal); writing – review and editing (equal). Céline Toty:

Investigation (equal); writing – review and editing (equal). Avril Duchet: Investigation (equal); writing – review and editing (equal). Léa Joffrin: Investigation (equal); writing – review and editing (equal). Riana V. Ramanantsalama: Investigation (equal); writing – review and editing (equal). Pablo Tortosa: Funding acquisition (equal); investigation (equal); writing – review and editing (equal). Patrick Mavingui: Supervision (equal); writing – review and editing (equal). Muriel Dietrich: Conceptualization (lead); formal analysis (equal); funding acquisition (equal); investigation (lead); supervision (equal); validation (lead); writing – original draft (equal); writing – review and editing (equal).

Competing Interest Statement:

We have no competing interests to declare.

Keywords

bats; tropical island; co-shedding dynamics; ecological factors; persistent shedding

Short title

Drivers of co-shedding dynamics in bats

Abstract

Understanding processes driving pathogen transmission in bats is critical to prevent spillovers and emergence events. Although substantial research has addressed this topic, few studies have directly examined shedding dynamics (as opposed to serological studies) and co-infection patterns using fine-scale spatio-temporal datasets. Here, based on the monitoring of 5,714 Reunion free-tailed bats (*Mormopterus francoismoutoui*) in 17 roosts over 24 months, we studied the co-shedding dynamics of paramyxoviruses (PMV) and *Leptospira* bacteria (LEPTO) in urine, and herpesviruses (HSV) in saliva. We evidenced all year long shedding with high prevalence of all three infectious agents (37% - 87%), as well as an exceptionally high level of co-shedding (59%), with both positive and negative interactions between infectious agents. Shedding patterns displayed temporal synchrony among roosts, with a peak during summer months, but were not influenced by roost size. Repeated shedding in recaptured bats supports within-host persistence, though underlying mechanisms remain to be identified. Our results also showed rapid HSV infection of juveniles (< 6 months), and suggest longer protection of juveniles by maternal antibodies for PMV and LEPTO. Reproductive individuals (both during the pregnancy and mating) were associated to increased PMV and LEPTO shedding, which can result from tradeoffs between reproduction and infection in both sexes, and/or an age-related bias with the progressive infection of older juveniles during reproductive periods. This study highlights the significance of persistent shedding of multiple pathogens, including bacteria, and their intricate interactions within bat populations. Understanding how human-driven ecological changes may disrupt within-host processes and influence pathogen shedding in bats will help assessing the risk of pathogen spillover from bats to other species, including humans.

Author summary

Understanding risks of bat-borne pathogen spillover is challenging because of the difficulty in studying shedding dynamics in wild bat populations. Here, we used an original island-endemic bat species to build up a fine-scale spatio-temporal shedding analysis of two viruses (paramyxoviruses and herpesviruses) and a bacterium (*Leptospira*) at both population- (roost) and individual- (through recaptured bats) levels. Shedding patterns are driven by the age of bats and associated to the reproductive periods in both females and males. Results also suggest that persistence, as well as interactions between infectious agents, are important within-host processes that contribute to the transmission of infections in bat populations. More research is essential to understand how human activities may influence these co-shedding patterns and the risk of cross-species transmission.

Introduction

Several human outbreaks, such as those caused by the SARS-CoV-1 and Nipah viruses, have highlighted the importance of understanding processes driving the transmission of infectious agents within bat populations [1]. Indeed, infection dynamics in bat reservoir hosts have been linked to zoonotic spillovers [2, 3]. Thus, identifying the ecological drivers of pathogen transmission within bat populations, at both within- and between-host levels, is a key element for predicting spillover events [4, 5]. Unfortunately, ecological studies investigating infection dynamics in bats often lack robust spatio-temporal datasets [6] (but see e.g. [7-10]). This gap mainly results from logistical constraints due to the elusive and roaming nature of bats that make these animals difficult to study over long periods, and limits the breadth of data acquisition. Moreover, these gregarious mammals often display metapopulation dynamics [11]. Such spatio-temporal heterogeneity is characterized by periodically interacting spatial discrete patches, with various sex and age-structure, roost size and function [12, 13], which adds complexity to disentangle individual and populational drivers of infection dynamics in bats [8, 14, 15].

With molecular tools becoming increasingly accessible for the study of infectious agents, it is now recognized that co-infections are common in bats [16–20]. However, most of the previous longitudinal studies on bats have focused on a single infectious agent, or different viral species within the same family (e.g. [2, 21–23]). Thus, our knowledge on spatio-temporal co-infection dynamics with different groups of infectious agents (DNA/RNA viruses, bacteria, fungi) remains limited [10, 24–26]. Theory predicts that co-infections can have major consequences on within-host infection dynamics because of potential interactions that might be antagonistic or mutualistic [19, 27, 28]. For example, the infection of field voles with the bacterium *Anaplasma phagocytophilum* increased by five times the susceptibility to cowpox virus [29]. Examining the spatio-temporal patterns of simultaneous shedding of infectious agents within bat roosts (co-circulation) and individual hosts (co-infection) is likely to provide much-needed further insights into underlying processes driving infection dynamics [2].

113 Islands are widely considered as relevant model systems in ecology and
114 evolutionary biology studies [30, 31], including those focusing on emerging diseases (e.g.
115 [32, 33]). These ecosystems typically support a limited number of species and exhibit high
116 levels of endemism [34]. Due to their ability to fly over water, bats are often the only
117 native mammals in remote oceanic islands. Among the 1,456 recognized bat species, 60%
118 inhabit islands and 25% are even island-endemic [35]. The clearly defined geographical
119 boundaries and often reduced surface of islands enable sampling endemic bat
120 populations at a fine scale, by focusing sampling efforts on a specific limited area which
121 covers a comprehensive range of sites, and this is crucial to make reliable inferences
122 about spatial and temporal infection dynamics [36]. Moreover, the reduced number of
123 bat species on islands may also simplify ecological interactions, by minimizing interspecies
124 contacts, and by sampling monospecific bat roosts, which can contribute to a more in-
125 depth understanding of infection dynamics at the population level [37]. Due to the
126 reduced species richness typical of small territories, insular ecosystems may also lack
127 predators or competitors and offer empty ecological niches, which can favor the spread
128 of island endemic bats and the expansion of their population size, although this would
129 ultimately be constrained by the availability of resources. This is especially true for bat
130 families with highly gregarious behavior such as free-tailed bats (Molossidae), for which
131 roosts can host hundreds of thousands of individuals [38, 39]. High bat densities favor the
132 sampling of large numbers of individuals, a prerequisite for epidemiological studies. Island
133 endemic bats, with such an abundant, simplified, and well-defined system, represent a
134 rare opportunity to collect extensive spatio-temporal data to capture a comprehensive
135 picture of subtle mechanisms underlying infection dynamics in bats [37].

136 The Reunion free-tailed bat (*Mormopterus francoismoutoui*; [40]) is a small
137 tropical insectivorous bat endemic to Reunion Island. This volcanic territory is located in
138 the southwestern Indian Ocean and emerged about 3 million years ago [41]. Although
139 small in size (2,512 km^2), Reunion Island is shaped by a mountainous landscape and has
140 undergone significant landscape changes following 350 years of human colonization
141 associated with intensive urbanization and agriculture [42]. Reunion free-tailed bats are

142 broadly distributed on the island and monospecific roosts occur in a diversity of natural
143 habitats, such as caves and cliffs. These mollosid bats have also adapted to urbanization
144 and use numerous anthropogenic roosts such as buildings and bridges, hosting from a
145 few hundred to more than 100,000 individuals [12, 40]. A recent longitudinal monitoring
146 of several roosts revealed highly dynamic roosting behaviors, with roosts of various sizes,
147 sex-ratio, and functions (female-biased maternities, mixed colonies or male-biased
148 roosts) [12]. Specifically, large female aggregations (up to 50,000 pregnant females) are
149 observed synchronously every year in a few roosts, before parturition in austral summer
150 (December), which coincides with a female-biased sex-ratio and a spatial sexual
151 segregation during this period of the year [12, 43]. Moreover, the end of austral summer
152 (May) is characterized by a decrease in roost size and a change in sex-ratio in the studied
153 roosts (from female- to male-biased), suggesting important seasonal sex-specific
154 movements within the island, which is corroborated by the absence of spatial genetic
155 structure in this metapopulation [44].

156 Reunion free-tailed bats are natural hosts for several infectious agents [10, 21,,
157 45], including paramyxoviruses and *Leptospira* bacteria [43]. Previous non-invasive
158 sampling of bat faeces and urine underneath roosts highlights that shedding pulses of
159 paramyxoviruses and *Leptospira* bacteria occurred during the austral summer, followed
160 by a sustained transmission during winter [10, 43, 45]. However, these studies relied on
161 a reduced number of samples that did not include information on individual bats (as no
162 captures were performed), precluding direct insights into how individual factors (e.g. sex,
163 age, reproductive status) influence these shedding dynamics. Moreover, studies were
164 conducted on only two maternity roosts [10, 43] and the role of population-level factors
165 (e.g. roost size, sex-ratio) thus remains poorly understood. Here, we used data from a
166 fine-scale spatio-temporal monitoring and sampling of *M*. *francoismoutoui*, based on the
167 study of 17 roosts all over Reunion Island during two consecutive years. We measured
168 the simultaneous shedding (nucleic acid detection) of three infectious agents in each
169 individual bat, focusing on paramyxoviruses (viral RNA) and *Leptospira* (bacteria DNA)
170 both shed in urine, and herpesviruses (viral DNA) in the saliva. Specifically, we first aimed

171 to test for spatio-temporal trends in shedding prevalence and synchrony across roost
172 sites. Then, we evaluated whether individual (sex, age, reproductive status) and roost-
173 level (roost size and level of sexual spatial segregation) variables explained prevalence of
174 single infectious agents, co-shedding patterns, and the probability of changing shedding
175 status (within-host dynamics).
176

177 ## Results

178 **Spatio-temporal dynamics of shedding prevalence.**

179 Between January 2019 and December 2020 (24 months), we captured 5,714 Reunion
180 free-tailed bats in 17 roosts all over Reunion Island (Fig 1), including 405 recaptures (up
181 to four recaptures were recorded for the same individual). Shedding data were obtained
182 from 5,518 urine samples for paramyxoviruses (PMV) and *Leptospira* bacteria (LEPTO),
183 and from 3,981 saliva samples for herpesviruses (HSV), including 3,784 individuals for
184 which all three infectious agents were tested. Over the entire study period, we measured
185 a high global prevalence with 36.63% ± 1.27% of bats shedding PMV, 46.48% ± 1.32%
186 shedding LEPTO and 87.14% ± 1.04% shedding HSV (considering recaptured bats as
187 independent points in time) (Table 1).
188

189 **Table 1. Details on the sampled roosts of *M. francoismoutoui* and the number of tested**
190 **and positive samples.**
191

Roost	Habitat	No. of sampling periods	Roost size estimation (min and max when available)	No. of urine tested	No. of PMV positive (%)	No. of LEPTO positive (%)	No. of saliva tested	No. of HSV positive (%)
AOM	Building	1	2560	52	6 (11.5)	10 (19.2)	0	no data
EGI	Building	3	no data	149	56 (37.6)	79 (53.0)	89	82 (92.1)
ESA	Bridge	15	570 - 3200	634 (PMV) 635 (LEPTO)	254 (40.0)	360 (56.7)	452	406 (89.9)
MON	Bridge	15	210 - 1150	488	144 (28.4)	268 (54.9)	419	355 (84.5)
PBV	Cliff	1	300	11	4 (36.4)	8 (72.7)	0	no data
PSR	Building	15	no data	512 (PMV) 510 (LEPTO)	255 (49.8)	305 (59.8)	396	387 (97.8)
PSR-SUD	Building	1	no data	51	9 (17.6)	14 (27.4)	0	no data
RBL	Bridge	15	350 - 1300	658	238 (36.2)	235 (35.7)	425	369 (86.8)
RES	Bridge	8	35 - 410	223	91 (41.0)	111 (49.8)	212	179 (84.4)
RPQ	Bridge	15	150 - 3000	535 (PMV) 536 (LEPTO)	229 (41.9)	287 (53.4)	416	386 (92.8)
STJ	Building	1	200	34	14 (41.2)	10 (29.4)	0	no data
STM	Bridge	12	27 - 350	364	145 (39.9)	166 (45.6)	281	267 (95.0)
TBA*	Cave	11	0 - 100,000	500	140 (28.0)	168 (33.6)	330	217 (65.8)
TGI*	Building	15	75 - 1270	496	167 (33.7)	229 (46.1)	432	356 (82.4)
TM5	Bridge	1	200	28	0	4 (14.3)	0	no data
TRI	Bridge	4	153 - 251	125	45 (36.0)	86 (68.8)	112	104 (92.9)
VSP	Bridge	15	15 - 6000	658	224 (34.0)	225 (34.2)	417	361 (86.6)
Total	/	/	/	5,518	2,021 (36.6)	2,565 (46.5)	3,981	3,469 (87.1)

192
193
194 Shedding of the three infectious agents was detected in all tested roosts, except PMV in
195 the TM5 roost (temporary roost exclusively composed of juveniles; see [12]). Pairwise
196 comparison of prevalence among roosts at different sampling periods (calculated as
197 Pearson's correlations) revealed both positive and negative correlation coefficients, and
198 thus a moderate level of spatial synchrony, which was slightly higher for HSV (regional
199 synchrony = 0.269) compared to PMV (regional synchrony = 0.151) and LEPTO (regional
200 synchrony = 0.202). Moreover, spline correlograms showed that synchrony was not
201 influenced by the geographical distance between roosts (Fig 2A). A dynamic factor
202 analysis (DFA) was then used to model common trends in prevalence across roosts.
203 Despite variation of prevalence patterns among roosts (Fig 2B), DFA models converged
204 and showed a common trend that peaked during the summer months (from October to
205 December) for the three infectious agents, and then reached its lowest around March to

June (Fig 2C). Roost loadings varied only substantially in both magnitude and direction. In particular, the roosts MON, RPQ and TGI showed the lowest loadings (sometimes negative) which implies some degree of asynchrony for these roosts. Finally, the use of generalized additive models (GAM) (S1 and S3 Tables), to characterize variation in prevalence, confirmed significant intra-annual variations for PMV and HSV prevalence (model M1: $\chi^2_{5.7} = 15.05$, $P = 0.03$; model M3: $\chi^2_{6.7} = 19.86$, $P = 0.01$; S1 Table).

Roost-level drivers of shedding.

Roost size varied from 15 to 100,000 individuals but was not correlated with the prevalence of PMV and LEPTO (model M1: z = 0.37, $P = 0.71$; model M2: z = 0.80, $P = 0.43$; S1 Table), while HSV prevalence slightly decreased in larger roosts (model M3: z = -2.83, $P = 0.005$; S1 Table). However, this negative correlation was driven by the presence of juveniles when roost sizes were the highest, these juveniles being low infected (see after). This negative correlation disappeared when juveniles were removed from the HSV model (model M3bis: z = -0.83, $P = 0.41$; S1 Table). Because adult males and females aggregate and segregate differently among roosts [12], we also examined the role of sexual segregation levels of adults, but did not find any correlation with prevalence (model M1: $\chi^2_{4.3} = 1.55$, $P = 0.90$; model M2: $\chi^2_{2.9} = 1.76$, $P = 0.60$; model M3: $\chi^2_{4.9} = 7.38$, $P = 0.40$; S1 Table).

Individual variation of shedding.

Models revealed that adults were systematically more frequently shedding viruses and bacteria than juveniles (model M1: z = -5.83, $P = 5.62^{-09}$; model M2: z = -6.17, $P = 6.73^{-10}$; model M3: z = -11.88, $P < 2^{-16}$; S1 Table). Moreover, for *Leptospira* bacteria that was detected using a real-time PCR, we analyzed the cycle threshold (Ct) values which serve as a proxy for bacterial load. The model indicated that, when infected, juveniles shed a significantly lower *Leptospira* load compared to adults (model M4: z = 11.78, $P < 2^{-16}$; S1 Table).

234 Mean shedding prevalence in adults was high: 43.00 ± 1.42% for PMV, 52.85 ±
235 1.43% for LEPTO and 96.20 ± 0.65% for HSV (Figs 3A- C). In contrast, at the time when
236 juveniles started to fly (January-February; [12]), shedding prevalence in juveniles was
237 either null (PMV) or low (LEPTO: 12.03 ± 4.11% and HSV: 15.03 ± 5.66%). Then, over the
238 following six months, HSV prevalence increased drastically in juveniles to reach 60.67 ±
239 7.82%, while it remained close to 0% for PMV, or only slightly increased for LEPTO (Figs
240 3A-C). After six months, we could not monitor properly infection in juveniles because
241 most of bats were classified as adults based on the epiphysis fusion, but we noted that
242 for females with non-developing nipples (M0 females; that probably include juveniles),
243 PMV and LEPTO infection remained low for at least 6 more months (S1 Fig). Shedding
244 prevalence also varied according to sex, but only in adult bats, and differently according
245 to the targeted infectious agent (model M1: z = -5.03, $P = 4.81^{-07}$; model M2: z = -0.77, P
246 = 0.44; model M3: z = 3.84, $P = 1.25^{-04}$; S1 Table) (Figs 3D -F). Indeed, adult males were
247 more frequently shedding HSV than females (Tukey's post hoc test: t = -3.84, $P = 7.0^{-04}$),
248 although the opposite pattern was observed for PMV (Tukey's post hoc test, t = 5.03, $P <$
249 1.0^{-04}).
250 To test the influence of reproduction on the shedding status, we focused our
251 analysis on adults during two reproductive periods: pregnancy (November-December)
252 and mating (March-April). During pregnancy, the detection of the two urine-excreted
253 agents, PMV and LEPTO, was higher in pregnant than in non-pregnant females (model
254 M5: z = 5.76, $P = 8.31^{-09}$; model M6: z = 5.20, $P = 2.02^{-07}$; S2 Table) (Figs 3D-E). However,
255 when we excluded non-pregnant females with no visible nipples (M0) from the models—
256 potentially representing misclassified old juveniles—the effect of pregnancy was no
257 longer detected (model M5bis: z = 0.72, P = 0.47; model M6bis: z = 1.35, P = 0.18; S2
258 Table) (Fig 3D -E). Moreover, during November-December, non-pregnant females without
259 visible nipples were indeed less frequently infected compared to non-pregnant females
260 with visible nipples, regardless of pregnancy status (S1 Fig). For males, during the mating
261 period, reproductively active individuals were more frequently found shedding LEPTO
262 than non-reproductive males (model M10: z =2.70, P = 0.007; S2 Table) (Fig 3E). Finally,

263 we did not find any influence of reproduction of the *Leptospira* load (Ct) for both females
264 and males (model M7: z = -1.69, P = 0.09; model M11: z = 1.62, P = 0.11; S2 Table).
265
266 **Co-shedding dynamics.**
267 Among the 3,784 bats with paired samples (both urine and saliva collected), 36.89% (n =
268 1,396) were shedding two infectious agents and 22.46% (n = 850) were shedding three
269 (S2 Fig). Only 399 bats (10.54%) did not excrete any of the three screened infectious
270 agents, with 79.2% of them being noteworthily juveniles. Shedding one infectious agent
271 increased the probability of shedding a second infectious agent (for all combinations in
272 models M1, M2, M3, all $P < 0.001$; S1 Table) (Fig 4). The relationship between viral
273 infections was stronger than that between viruses and bacteria. For example, based on
274 odd ratios estimated from models M1-M3, bats shedding HSV were 14 times more likely
275 to shed PMV, whereas shedding HSV increased the likelihood of LEPTO shedding only by
276 threefold. Additionally, individuals already shedding two infectious agents were more
277 likely to shed a third (Fig 4). However, in cases of triple infections, a negative interaction
278 was observed, indicating that the combined effect of two agents on the prevalence of the
279 third was weaker than expected if the two infections were independent (model M1: z = -
280 3.10, P = 0.002; model M2: z = -2.46, P = 0.01; model M3: z = -2.51, P = 0.01; S1 Table).
281 Models showed no significant intra-annual variations for dual and triple shedding,
282 except for PMV-HSV (model M15: $\chi_{5.7}$ = 17.46, P = 0.01; S3 Table), and no effect either of
283 sexual segregation or roost size. By contrast, we detected a strong influence of age, with
284 dual and triple shedding being more frequent in adults (model M13: z = -4.73, $P = 2.30^{-06}$;
285 model M14: z = -10.67, $P < 2^{-16}$; model M15: z = -7.39, $P = 1.43^{-13}$; model M16: z = -4.69,
286 $P = 2.68^{-06}$; S3 Table), especially in adult females (Tukey's post hoc test, model M13: t =
287 5.04, $P < 0.001$; model M15: t = 4.26, P = 0.001). Finally, pregnancy increased the
288 probability of dual and triple shedding in females (model M17: z = 4.01, $P = 6.15^{-05}$; model
289 M18: z =4.93, $P = 8.05^{-07}$; model M19: z = 5.07, $P = 3.97^{-07}$; model M20: z = 3.79, $P = 1.5^{-}$
290 ^{04}; S4 Table), but when non-pregnant females without visible nipples (M0) were excluded,
291 this effect was no longer observed (S4 Table). In males, reproductively active individuals

292 had a higher probability of simultaneously shedding LEPTO and HSV compared to the non-
293 reproductive ones (model M22: z = 2.66; *P* = 0.008; S4 Table).
294
295 **Within-host dynamics of shedding.**
296 All captured bats were marked (by tattooing on the wing) allowing to collect shedding
297 data at the individual level. We tested 471 and 457 samples for PMV and LEPTO
298 respectively, including initial capture and samples from recaptured bats. We also tested
299 86 saliva samples from 31 recaptured bats (from 2 to 5 capture events) for the presence
300 of HSV. All bats initially testing HSV-positive (n = 29) remained positive over time
301 (between 25 and 405 days between recapture events), while the only two initially-
302 negative bats were found to be positive at their first recapture. Thus, within-host analyses
303 using multinomial logistic regressions of shedding status transitions were only performed
304 on PMV and LEPTO data. Recapture intervals ranged from 25 to 719 days (S3A Fig), during
305 which we defined four transition classes: negative to negative (no transition), negative to
306 positive, positive to negative, and positive to positive (no transition). A significant
307 proportion of recaptured bats maintained their initial shedding status over time.
308 Specifically, 50.74% (PMV) and 40.04% (LEPTO) of recaptured bats remained negative,
309 while a smaller yet notable fraction (PMV: 25.69%, LEPTO: 34.79%) consistently remained
310 positive. Notably, among initially-positive bats, approximately 75% remained positive
311 over time, though this percentage slightly declined for PMV when bats were recaptured
312 after 12 months (Fig 5A). Examples of bats that remained positive throughout multiple
313 recapture events, both within the same year (short-time intervals) and across different
314 years (long-time intervals) are illustrated in S4 Fig.
315 The probability of the four shedding status transitions was significantly dependent
316 on the time interval between recaptures for LEPTO (model M25, S5 Table) (Fig 5B), but
317 not for PMV (model M26, S5 Table) (Fig 5C). Indeed, the probability of shedding LEPTO
318 (either negative to positive, or positive to positive) increased with time interval, while the
319 probability of stopping shedding LEPTO (positive to negative) remained low and stable
320 (Fig 5B). We also found a significant effect of changing reproductive status on the

321 probability of changing both PMV and LEPTO shedding status (models M5 and M26, S5
322 Table). Indeed, bats that remained non-reproductively active over recapture events
323 (reproduction transition: 0/0), also mainly remained LEPTO- and PMV-negative (shedding
324 transition: 0/0) (Figs 5D and E). Similarly, most bats successively captured when
325 reproductively active (reproduction transition: 1/1) remained LEPTO- and PMV-positive
326 (shedding transition: 1/1).
327

328 **Discussion**

329 Using an original island-endemic bat system, we demonstrated the widespread and all-
330 year-long co-shedding of two viral and one bacterial agents in Reunion free-tailed bat
331 populations. This confirms the circulation of PMV and LEPTO [10, 43] and describes for
332 the first time HSV in this bat species. We revealed high global prevalence of PMV (37%)
333 and LEPTO (46%), and extremely high prevalence of HSV (87%), which contrasts with
334 certain other bat-borne infectious agents, such as Henipaviruses, Filoviruses, and
335 Lyssaviruses, where viral shedding is infrequently detected (e.g. [6, 46]). Our nearly
336 complete HSV prevalence aligns with the consistently high HSV rates observed in other
337 bat species, such as in the Mexican free-tailed bat *Tadarida brasiliensis* [47] and in the
338 common vampire bat *Desmodus rotundus* [14, 48]. High shedding prevalence in Reunion
339 free-tailed bats could be explained by a strong gregarious behaviour of these bats, which
340 can aggregate up to 1500 adult individuals per m^2 [49]. The proximity of individuals within
341 roosts can facilitate transmission through bat fluids (saliva, urine), in which case, roost
342 size is often assumed to positively correlate with prevalence [50–52]. However, we did
343 not find such a correlation, suggesting that roost size may not play a major role in the
344 shedding of paramyxoviruses, *Leptospira* and herpesviruses in Reunion free-tailed bats.
345 This aligns with previous findings on coronavirus in these bats, which demonstrated
346 similar dynamics in two maternity colonies with markedly different roost sizes [10].
347 Moreover, we observed a degree of spatial synchrony between roosts, with a common
348 prevalence trend characterized by consistently high prevalence throughout the year, and
349 an increase during the summer months. These correlated shedding dynamics were

350 observed even between geographically distant roosts. The high prevalence in our current
351 dataset, as well as the low variability across sampling periods, may have obscured a higher
352 signal of detectable synchrony. Extending the time series could provide the necessary
353 variation and statistical power to capture any underlying synchronous trends across
354 roosts and confirm our initial conclusions. Although frequent intra- and inter-seasonal
355 movements is suspected in Reunion free-tailed bats [12, 44], potentially contributing to
356 pathogen spread and spatial synchrony, our results suggest that transient epidemics,
357 marked by waves of bat-to-bat transmission between roosts, are not the primary
358 mechanism driving global PMV, LEPTO and HSV shedding dynamics [8, 50, 53]. Instead,
359 intrinsic biological cycles, which are influenced by individual (reproductive status, age,
360 and immune function) and environmental factors (e.g., food availability, temperature)
361 could create synchronized shedding patterns among roosts [5, 50].

362 Several studies have reported that age structure within bat populations is a critical
363 determinant of infection dynamics [5]. For coronaviruses, studies have documented
364 higher infection rates among juveniles, who become rapidly infected shortly after birth
365 [9, 10, 21]. In our study, the rapid increase in HSV infections (60% of infection in 4-months
366 old juveniles) suggests a similar rapid waning of maternal immunity. In contrast, juveniles
367 showed relatively low infection rates for PMV and LEPTO during their first six months of
368 life. Additionally, observations of females with non-developing nipples, which were
369 associated with low infection rates (S1 Fig), suggest that older juveniles may remain
370 protected against PMV and LEPTO for an extended period. While we could not confirm
371 this timing explicitly because of the incertitude in aging old juveniles, this is consistent
372 with the longer maternal immunity reported in field and modelling studies for Lagos bat
373 virus, henipaviruses and Marburg virus (e.g. 37, 54–57]. Further serological investigations
374 are thus required to determine the duration of maternal antibodies in this bat species.

375 Behavioral and physiological traits are two mechanisms that can produce sex-
376 biased prevalence in several wildlife species [58, 59]. Here, adult males were more
377 frequently shedding HSV than females, as previously reported in rodents [60] or for other
378 DNA bat viruses such as adenoviruses [61]. In contrary, adult females were more

379 frequently shedding PMV. Studies on HSV prevalence in bats are limited and report
380 contrasting results, with no sex difference in *D. rotundus* [14], while Sjodin et al., [62]
381 suggest that either males or females can be more infected, depending of the herpesvirus
382 strain. Male-biased infection may arise from sex-specific social behaviour like dominance
383 or higher aggressiveness (physical injuries, i.e. bite) [63, 64], that could enhance
384 transmission in males [60, 65]. Sex hormones can also strongly affect host susceptibility,
385 through the modulation of immunity [66]. Testosterone may suppress immune responses
386 in males, increasing susceptibility to pathogen infection [67]. The inclusion of hormone
387 and immunity measures should thus be considered in future infection studies to test this
388 hypothesis in bats.

389 At the individual level, chronic or episodic shedding from persistently infected bats
390 can lead to high prevalence across roosts and time [4]. However, deciphering between
391 the different within-host processes that may lead to such persistence can be challenging.
392 For HSV, in addition to an extreme high prevalence, our recapture data showed that all
393 initially HSV-positive bats were still shedding HSV in saliva over recaptures, supporting
394 indeed lifelong HSV infection in Reunion free-tailed bats. HSV are known to establish
395 latent infection in humans [68] and rodents [60], and the same mechanism is also
396 suspected in bats [69, 70]. Interestingly *in D. rotundus* infected with a betaherpesvirus
397 [14], the length of the active period (when shedding occurs) appears to be longer than
398 the latency state (when shedding resumes) [70]. The same mechanism of latency and long
399 phase of active shedding could explain our result, although we cannot exclude continuous
400 shedding from persistent infections. The recent deep sequencing of HSV-positive samples
401 collected over three consecutive years—including some samples analyzed in this study—
402 identified co-infections of Reunion free-tailed bats with multiple strains spanning three
403 HSV subfamilies (alpha, beta, and gamma) [71]. These findings also indicated a low
404 probability of strain loss over time, supporting within-host persistence. To distinguish
405 between within-host processes contributing to HSV persistence in Reunion free-tailed
406 bats, further sequencing efforts will be necessary to uncover potential subfamily- or
407 strain-specific dynamics [48]), which may be masked within the global HSV shedding

408 prevalence observed in the present study. This has, for example, been recently shown for
409 distinct bat-borne coronavirus and paramyxovirus lineages [2, 23, 72].

410 For PMV and LEPTO, our extensive dataset of recaptured bats revealed that
411 approximately 75% of initially positive individuals continued to shed viral RNA and
412 bacterial DNA in their urine over extended periods. Additionally, examples of bats
413 remaining positive across multiple recapture events further support the hypothesis that
414 persistent infections contribute to the observed temporal dynamics of PMV and LEPTO.
415 However, we also observed transitions from positive to negative shedding for PMV and
416 LEPTO, indicating that cycles of clearance followed by reinfection may occur within the
417 bat population, although the possibility of recrudescence from latent infections cannot
418 be ruled out. Persistent LEPTO infection in bats is not surprising as this bacterial infection
419 is often considered chronic in other reservoir hosts, bacteria forming protective biofilms
420 in renal tubules [73]. Experimental infections have shown that *Leptospira interrogans* can
421 stably colonize the kidneys of rats and mice over their lifespan, with intermittent shedding
422 of the bacteria that can last for at least 3 months [74, 75]. Our data showed that when
423 individuals were shedding LEPTO upon their first capture, the probability of stopping
424 shedding was low and stable over time, which is in keeping with an intermittent shedding.
425 On contrary, mechanisms underlying within-host PMV dynamics are still debated [4, 76].
426 Several field and lab evidence support that henipavirus, for example, can persist within
427 individual bats, with long-term shedding occurring either continuously or intermittently
428 through recrudescence [8, 37, 77–80]. A modelling study also suggests that latent
429 henipavirus infections can occur alongside occasional viral clearance, followed by
430 temporary immunity and reinfection [76]. This same study supports that bats are much
431 more likely to develop a latent infection than clearing it. Finally, it has been hypothesized
432 that a small portion of super-long-shedder individuals with a long infectious period could
433 maintain Hendra virus in bat populations [81]. Distinguishing between these different
434 infection processes is complex. Because we only measured the presence of viral and
435 bacterial nucleic acids in our study, a first step will be to assess the infectiousness of
436 excreted samples to finely validate the role of long-term continuous and intermittent

437 shedding in transmission [50]. Secondly, as we previously showed the presence of several
438 paramyxovirus variants in Reunion free-tailed bats, but only one for *Leptospira* [43],
439 further sequencing of positive samples from this study will be necessary to assess
440 temporal dynamics at a finer taxonomic scale, and provide key information on viral and
441 bacterial evolution within the bat host [4]. Together with further development of
442 epidemiological models [82], such genetic data will help clarify the mechanisms shaping
443 the observed shedding dynamics (e.g. [7, 8, 70, 76]).

444 In persistent infections, the reactivation process is often linked to several stressors
445 that may affect host immunity [83, 84]. Reproduction, by imposing immunological
446 challenges, is recognized as a major stressor that could lead to the reactivation of viral
447 and bacterial shedding [85]. Such processes are expected to be particularly pronounced
448 in female mammals, for whom reproduction requires large and prolonged energetic
449 investments [86, 87]. Although less documented, male reproduction trade-offs have also
450 been suggested in bats [88] and could be mediated by reduced immune function during
451 spermatogenesis, a period of high energy demand and elevated testosterone [89–91].
452 Our results suggest that pregnancy increases the probability of PMV and LEPTO shedding,
453 as well as the likelihood of dual and triple shedding in Reunion free-tailed bats. Moreover,
454 our study suggested that, during the mating period, reproductively active males had a
455 higher probability of shedding LEPTO (and LEPTO-HSV), as compared to non-reproductive
456 males. Individual recapture histories also suggest that changes in reproductive status
457 influence PMV and LEPTO shedding. The lack of effect for HSV is likely due to its high
458 prevalence, which may obscure any potential reproductive influence, as also observed in
459 HSV-infected *Rousettus aegyptiacus* and *Miniopterus natalensis* [92]. We thus
460 hypothesize that shedding could be reactivated during pregnancy and mating periods in
461 Reunion free-tailed bats, as reported in other bat species [10, 21, 22, 43, 92, 93]. Such a
462 process, besides conferring protection to newborns through the transfer of protective
463 maternal antibodies, could benefit the adults through a boost of immunity and could
464 therefore be critical in the maintenance of long-term immunity [94]. We also cannot
465 exclude a potential age-related effect to explain these patterns. Indeed, distinguishing

466 adult bats from old juveniles (> 6 months-old) in the field, based on morphology alone,
467 was particularly challenging in our study. This difficulty may have introduced bias into our
468 observations of increased prevalence at the end of winter and the subsequent peak
469 during gestation (October–December). Specifically, these trends could partly reflect the
470 progressive infection of older juveniles misclassified as adults. Similarly, during the mating
471 period (March–April), adult male groups may include some misclassified year-old
472 juveniles (approximately 15 months old) with lower infection rates. Finally, immigration
473 of infected bats may also play a role in transmission during late pregnancy especially, as
474 massive aggregations of bats occur at this time of the year with possible horizontal
475 transmission to non-immune bats [12].

476 Our investigation targeting multiple simultaneous infectious agents revealed a
477 high co-shedding of viruses and bacteria within the bat population, with 59% of bats
478 shedding at least two infectious agents. Bats shedding one virus or bacteria had
479 significantly more chance of shedding another one, with a strong association between
480 viral infections in particular. This corroborates previous results suggesting positive
481 interactions that could facilitate shedding of paramyxoviruses [2, 43] and coronaviruses
482 [18, 25]. In the study of Davy et al. [18], the stress of fungal infection by
483 *Pseudogymnoascus destructans* led to a reactivation of coronavirus replication in the little
484 brown bat *Myotis lucifugus*, and co-infection even increased the severity of White Nose
485 Syndrome, illustrating how multiple infections can interact to affect host health.
486 Interestingly, our study also found that dual infection also increased the likelihood of
487 shedding a third infectious agent, although combined effect of two infections on the third
488 was lower than expected. These interactions between infectious agents could modulate
489 host susceptibility in various ways, with both antagonistic and mutualistic effects,
490 depending on the community of infectious agents considered [29]. In our previous work,
491 we observed that coinfection with paramyxoviruses, coronaviruses and astroviruses was
492 a very rare event (1% of tested samples) in Reunion free-tailed bats and no significant
493 interactions were detected between these viruses [10]. This is probably explained by the
494 very low prevalence of astroviruses, and the timing of juvenile coronavirus infection,

495 which occurs between February and April [21], when they are still low infected by PMV.
496 These studies illustrate how considering simultaneously multiple infectious agents,
497 although complex, is important to better understand drivers of infection in bats [19, 95,
498 96]. Disruption of balanced host-pathogen relationships due to stressors, such as habitat
499 loss or co-infections, may increase pathogen shedding, and enhance the likelihood of
500 spillovers [3]. Further research exploring the dynamics of multi-infections in the context
501 of increasing urbanization, particularly in species like the urban-dwelling Reunion free-
502 tailed bat, will help in understanding how human-mediated changes in bat ecology may
503 affect natural shedding dynamics and ultimately the probability of spillovers [97].
504

505 ## Materials and Methods

506 **Study sites and field sampling**

507 We monitored and sampled 17 roosts (coded with a 3-letter code) from January 2019 to
508 December 2020 (24 months), all over Reunion Island (Fig 1). Among the 17 studied roosts,
509 12 were monitored across a maximum of 15 successive "sampling periods" occurring
510 every 3–8 weeks, each sampling period lasting for 3–4 weeks to be able to sample
511 multiple roosts (Table 1) (S6 Table). An opportunistic sampling was performed for five
512 additional roosts, which were thus monitored only once during the studied period. To
513 investigate within-host dynamics, we used data from recaptured bats, and thus also
514 included previously collected samples from 2018 (referred to as the first capture
515 samples).

516 Bat monitoring includes bat capture, biological sampling and roost size estimation
517 and is fully described in Aguillon et al. [12]. Captures were carried out using harp traps
518 (Faunatech Ausbat) and Japanese monofilament mist nets (Ecotone) during dusk
519 emergence, with a maximum of 60 individuals captured per night. Bats were hydrated
520 immediately after the capture and kept individually in a clean individual bag hang close
521 to a warm water bottle. For each bat, we measured the forearm length and mass, and
522 determined the sex, age, and reproductive status. Age was established by examining the

523 epiphysis fusion in finger articulations that are not welded for juveniles which was easily
524 identifiable from January to July, while some older juveniles might have been classified as
525 adults in the following months. In females, we recorded the development of nipples as
526 M0 for non-visible nipples, M1 for visible nipples, M2 inflated nipples (lactating), and M3
527 (visible nipples with regrowth of hair, post-lactating). Active reproductive status was
528 reported when females were pregnant (also verified by palpation of the abdomen),
529 lactating and post-lactating, and in males when they had large testes (see [12] for more
530 details). A sterile swab (Puritan Medical Products, USA) was carefully inserted in the
531 corner of the lips to sample saliva and then placed in 250uL of MEM (Minimum Essential
532 Medium Eagle). Using a pipette and a sterile tip, urine droplets were collected in the
533 waterproof bag or directly at the urethral opening when handling bats, and then placed
534 in 50 µL of MEM. All samples were stored in a cooled box in the field before being
535 transferred at -80°C at the laboratory the same night. Finally, each bat was tattooed on
536 the right propatagium with an individual alphanumeric code [98] and released at the
537 capture site.

538 Bats were handled using personal protective equipment regularly changed and all
539 the equipment was disinfected between sites (more details in [12]). Bat capture and
540 manipulation protocols were evaluated by the ethic committee of Reunion Island (CYROI,
541 n°114), and approved by the Minister of Higher Education, Research and Innovation
542 (APAFIS#10140-2017030119531267), and conducted under a permit delivered by the
543 Direction de l'Environnement, de l'Aménagement et du Logement (DEAL) of Reunion
544 Island (DEAL/SEB/UBIO/2018-09).

545

546 **Molecular detection of infectious agents**

547 Urine and saliva samples were processed using the Cador Pathogen 96 Qiacube HT kit
548 (Qiagen, Hilden, Germany), using 25 µL and 100 µL of samples, respectively, mixed with
549 175 µL and 100 µL of VXL buffer for the lysis step. Total nucleic acids were extracted using
550 an automated extractor Qiacube with small modifications of the Q Protocol using 350 µL
551 of ACB, 100 µL of AVE, and 30 µL of TopElute. A reverse transcription was then performed

552 on urine extracts [99], followed by the screening of paramyxoviruses and *Leptospira*
553 bacteria, using respectively a semi-nested PCR targeting the RNA polymerase gene of
554 Rubula-, Morbilli- and Henipa-virus genera, and a real-time PCR amplifying a fragment of
555 the 16S rDNA gene of several pathogenic *Leptospira* species [43, 100, 101]. For
556 paramyxoviruses, amplicons of the first PCR were diluted to 1:10, and 2 µL was then used
557 in the semi-nested PCR.

558 For saliva extracts, a fragment of herpesvirus DNA polymerase was amplified using
559 a nested PCR targeting a broad spectrum of herpesviruses (including α, β and γ sub-
560 families). During the first PCR, 2 µL of DNA was amplified in a 25 µL mixture containing
561 12.5 µL of GoTaq Green Master Mix 2X (Promega, Madison, Wisconsin, United States),
562 2.5 µL of each primer at 10 µM DFA (5'-GAYTTYGCNAGYYTNTAYCC-3') and KG1 (5'-
563 GTCTTGCTCACCAGNTCNACNCCYTT-3') [102]. We used the following thermal conditions:
564 95°C for 2 min, and 45 cycles at 94°C for 30 sec, 46°C for 1 min and 72°C for 1 min, and a
565 final step at 72°C for 7 min. During the nested PCR, 5 µL of amplificon was amplified in a
566 25 µL mixture containing 12.5 µL of GoTaq Green Master Mix 2X (Promega, Madison,
567 Wisconsin, United States), 2.5 µL of each primer at 10 µM TGV (5'-
568 TGTAACTCGGTGTAYGGNTTYACNGGNGT-3') and IYG (5'-
569 CACAGAGTCCGTRTCNCCRTADAT-3') [102]. We used the following thermal conditions:
570 95°C for 2 min, and 35 cycles at 94°C for 30 sec, 46°C for 30 sec and 72°C for 30 sec, and
571 a final step at 72°C for 7 min. PCR products were revealed using electrophoresis with 2%
572 agarose gel stained with 2% GelRed (Biotium, Fremont, USA).

573

574 **Statistical analyses**

575 We quantified the spatial (between roosts) synchrony in prevalence by calculating
576 Pearson's cross-correlations between the time series, for seven roosts (ESA, MON, PSR,
577 RBL, RPQ, TGI and VSP) that have complete temporal data (n=15 sampling periods). The
578 relation between synchrony and geographical distance was then modelled using the non-
579 parametric spatial covariance function Sncf in the *ncf* package [103], as in Paez [104]. For
580 that, we visually represented synchrony using spline correlograms, using a bootstrap

permutation test (n = 500 iterations) to generate 95% confidence intervals for the covariance function. Roosts sampled at least at eight different periods (n = 10) were used to fit the non-parametric correlation function, and missing data were handled via pairwise deletion of missing values for each pair of time series. Next, prevalence trends and synchrony were characterized using dynamic factor analysis (DFA) within the MARSS package [105]. Common trends were modeled by random walk, while loadings were estimated for each roost to describe the relationship between roost-specific time series and the common trend [106]. Time series were standardized to Z-scores (mean = 0, sd = 1) and modeled with a single common trend and an identity variance-covariance matrix.

To evaluate spatio-temporal shedding dynamics, we fit binomial generalized additive mixed models (GAM, [107]) via restricted maximum likelihood (REML) using the *mgcv* package (S1 and S3 Tables). We used penalized smoother for the temporal trend variable and controlled that the effective degrees of freedom (EDF) were higher than 1 (non-linear effect). The number of basis functions (k) and smooth parameters (alpha) were adjusted in each model using *gam.check* from the *mgcv* package to avoid overfitting and check for model convergence. Temporal trends were incorporated by assigning a numerical value to each sampling period, ranging from 1 (January-February) to 16 (November-December, S6 Table). Due to the COVID-19 crisis and the resulting lockdown in France, we did not monitor roosts in April 2020, and do not present data at that time. To properly account for the temporal effect, we decided to code the May-June 2020 sampling period as the middle of the notation used for March (coded as 10) and July 2020 (coded as 13, S6 Table). Final models for single, dual and triple shedding included the sampling period as smooth function, the roost size, age and sex (and their interaction) as linear function (S1 and S3 Tables). The significance of each modality of age/sex interactions was tested using a Tukey's post hoc test. For single shedding models, we also included the two other infectious agents, and their interaction, as a linear function. The influence of sexual spatial segregation patterns in adults on the prevalence was tested using the Sexual Segregation and Aggregation Statistic (SSAS, [108]). This statistic compares observed aggregation and segregation patterns to a random association of

610 males and females among roosts. We calculated SSAS values for each sampling period,
611 based on capture data reflecting the spatial distribution of individuals within roosts. The
612 SSAS was included in models, as a smooth function (details in S1 and S3 Tables). We also
613 assessed the difference in bacterial load of *Leptospira* between juveniles and adults by
614 including age as a predictor in a GLM, using the cycle threshold as a proxy for bacterial
615 load.

616 To assess the effect of reproductive status on shedding prevalence and bacterial
617 load (using cycle thresholds as a proxy), we focused on adult bats at two specific periods
618 of the year: firstly, in adult females during the pregnancy period (November-December)
619 to compare pregnant and non-pregnant adult females. We used a separate GLM on a
620 subset of data, for each sex, and included reproductive status as a linear effect (S2 and S4
621 Tables). During the pregnancy period, some non-pregnant females were classified as
622 adults, based on fused epiphyses, but lacked developed nipples (M0), which could
623 represent truly sexually mature adults that have not yet reproduced, as well as
624 misclassified sexually immature juveniles (about 11 months-old). To avoid including these
625 misclassified juveniles in the analysis, we ran the model both with and without the non-
626 pregnant M0 females. For males, our focus was on adult males during the mating period
627 (March-April), comparing reproductively active with non-reproductively active ones. It is
628 important to note that at this time of the year, males classified as adults may also include
629 some misclassified old juveniles (about 15 months-old) that could not be morphologically
630 distinguished [12].

631 To investigate within-host shedding dynamics, we tested the probability of
632 changing shedding status through time, by fitting a multinomial logistic regression using
633 the *multinom* function in the *nnet* package [109] (S5 Table). Because not enough HSV-
634 negative saliva samples were available to analyse transitions in HSV shedding status, we
635 only modelled transitions in shedding status for PMV and LEPTO. Changing shedding
636 status was used as a nominal dependent variable with four levels (negative to negative,
637 negative to positive, positive to negative, and positive to positive), with the following
638 covariates: recapture interval (in days), sex, and reproductive status transition (active to

active, non-active to active, active to non-active and non-active to non-active). Age classes were not included in the models because of the limited number of juveniles compared to adults (n_{JUV} = 29, n_{AD} = 497). This analysis used the non-changing shedding status, negative to negative, as a baseline outcome against which to compare other shedding status transitions. To better visualize the probable continuous shedding over time, we calculated and plotted the percentage of bats remaining positive for PMV and LEPTO across different time intervals: from < 4 months to > 16 months.

All analyses were performed in R.4.4.2 [110] using packages *dplyr*, *emmeans*, *lme4*, *ggeffects*, *ggplot2*, gridExtra, MARSS, *mgcv, ncf, reshape2, synchrony,* and *vegan*.

Acknowledgments

We are grateful to Eco-Med Océan Indien, Biotope, the DEER of Région Réunion (Direction de l'Exploitation et de l'Entretien des Routes), the DRT of Département Réunion (Direction des Routes et des Transports of the Department Reunion), and the City hall of Salazie for their help in identifying and accessing bat roosts. We are grateful to David Wilkinson for fruitful discussions. We also thank Clara Castex, Timothée Chenin, Jérémy Dubrulle, Marie Köster, and Guillaume Verchère for their assistance in the field.

Funding

This research was supported by the French National Research Agency (ANR JCJC SEXIBAT to MD) and by the European Regional Development Funds (ERDF PO INTERREG V ECOSPIR, number RE6875 to PT). SA and AOGH were supported by a "Contrat Doctoral de l'Université de La Réunion" from the Minister of Higher Education, Research and Innovation and LJ by an "Allocation Régionale de Recherche de la Région Réunion". The funders had no role in study design, data collection and analysis, decision to publish, or preparation of the manuscript.

Data Availability

Metadata are archived on Zenodo (https://doi.org/10.5281/zenodo.14842155). A pre-print is available on bioRxiv (https://doi.org/10.1101/2024.06.25.600581).

References

1. Letko M, Seifert SN, Olival KJ, Plowright RK, Munster VJ. Bat-borne virus diversity, spillover and emergence. Nat. Rev. Microbiol. 2020; 18: 461–471.

2. Peel AJ, Wells K, Giles J, Boyd V, Burroughs A, Edson D, et al. Synchronous shedding of multiple bat paramyxoviruses coincides with peak periods of Hendra virus spillover. Emerg. microbes & infect. 2019; 8: 1314–1323.

3. Becker DJ, Eby P, Madden W, Peel AJ, Plowright RK. Ecological conditions predict the intensity of Hendra virus excretion over space and time from bat reservoir hosts. Ecol. Lett. 2023; 26: 23–36.

4. Plowright RK, Peel AJ, Streicker DG, Gilbert AT, McCallum H, Wood J, et al. Transmission or within-host dynamics driving pulses of zoonotic viruses in reservoir–host populations. PLOS Negl. Trop. Dis. 2016; 10.

5. Sánchez CA, Phelps KL, Frank HK, Geldenhuys M, Griffiths ME, Jones DN,et al. Advances in understanding bat infection dynamics across biological scales. Proc. R. Soc. B: Biol. Sci. 2024; 291: 20232823.

6. Becker DJ, Crowley DE, Washburne AD, Plowright RK. Temporal and spatial limitations in global surveillance for bat filoviruses and henipaviruses. Biol. Lett. 2019; 15: 20190423.

7. Brook CE, Ranaivoson HC, Broder CC, Cunningham AA, Héraud J-M, Peel AJ, et al. Disentangling serology to elucidate henipa- and filovirus transmission in Madagascar fruit bats. J. Anim. Ecol. 2019; 88: 1001-1016.

8. Epstein JH, Anthony SJ, Islam A, A. Marm Kilpatrick A, Ali Khan S, Balkey MD, et al. Nipah virus dynamics in bats and implications for spillover to humans. Proc. Natl. Acad. Sci. U.S.A. 2020; 117: 29190–29201.

9. Cappelle J, Furey N, Hoem T, Putita Ou T, Lim T, Hul V, et al. Longitudinal monitoring in Cambodia suggests higher circulation of alpha and betacoronaviruses in juvenile and immature bats of three species. Sci. Rep. 2021; 11: 24145.

10. Hoarau AOG, Köster M, Dietrich M, Le Minter G, Joffrin L, Ramanantsalama RV et al. Synchronicity of viral shedding in molossid bat maternity colonies. Epidemiol. Infect. 2023; 151: e47.

700 11. Calisher CH, Childs JE, Field HE, Holmes KV, Schountz T. Bats: Important reservoir hosts of
701 emerging viruses. Clin. Microbiol. Rev. 2006; 19: 531–545.

702 12. Aguillon S, Le Minter G, Lebarbenchon C, Hoarau AOG, Toty C, Joffrin L, et al. A
703 population in perpetual motion: Highly dynamic roosting behavior of a tropical island
704 endemic bat. Ecol. Evol. 2023; 13: e9814.

705 13. Delpietro HA, Russo RG, Carter GG, Lord RD, Delpietro GL. Reproductive seasonality, sex
706 ratio and philopatry in Argentina's common vampire bats. R. Soc. Open Sci. 2017; 4:
707 160959.

708 14. Griffiths ME, Bergner LM, Broos A, Meza DK, da Silva Filipe A, Davison A, et al.
709 Epidemiology and biology of a herpesvirus in rabies endemic vampire bat populations.
710 Nat. Commun. 2020; 11: 5951.

711 15. Meza DK, Mollentze N, Broos A, Tello C, Valderrama W, Recuenco S, et al. Ecological
712 determinants of rabies virus dynamics in vampire bats and spillover to livestock. Proc. R.
713 Soc. B: Biol. Sci. 2022; 289: 20220860.

714 16. Anthony SJ, Epstein JH, Murray KA, Navarrete-Macias I, Zambrana-Torrelio CM, Solovyov
715 A, et al. A strategy to estimate unknown viral diversity in mammals. MBio. 2013; 4:
716 e00598-13.

717 17. Baker KS, K. S. Baker, Todd S, Marsh G, Fernandez-Loras A, Suu-Ire R, Wood JLN, et al. Co-
718 circulation of diverse paramyxoviruses in an urban African fruit bat population. J. Gen.
719 Virol. 2012; 93: 850–856.

720 18. Davy CM, Donaldson ME, Subudhi S, Rapin N, Warnecke L, Turner JM, et al. White-nose
721 syndrome is associated with increased replication of a naturally persisting coronaviruses
722 in bats. Sci. Rep. 2018; 8: 15508.

723 19. Hoarau AOG, Mavingui P, Lebarbenchon C. Coinfections in wildlife: Focus on a neglected
724 aspect of infectious disease epidemiology. PLOS Pathog. 2020; 16: e1008790.

725 20. Wang J, Pan Y-F, Yang L-F, Yang W-H, Lv K, Luo C-M, et al. Individual bat virome analysis
726 reveals co-infection and spillover among bats and virus zoonotic potential. Nat. Commun.
727 2023; 14: 4079.

728 21. Joffrin L, Hoarau AOG, Lagadec E, Torrontegi O, Köster M, Le Minter G, et al. Seasonality
729 of coronavirus shedding in tropical bats. R. Soc. Open Sci. 2022; 9: 211600.

730 22. Mortlock M, Dietrich M, Weyer J, Paweska JT, Markotter W. Co-circulation and excretion
731 dynamics of diverse rubula-and related viruses in Egyptian rousette bats from South
732 Africa. Viruses. 2019; 11: 37.

733 23. Geldenhuys M, Ross N, Dietrich M, de Vries JL, Mortlock M, Epstein JH et al. Viral
734 maintenance and excretion dynamics of coronaviruses within an Egyptian rousette fruit
735 bat maternal colony: considerations for spillover. Sci. Rep. 2023; 13: 15829.

736 24. Lane JK, Negash Y, Randhawa N, Kebede N, Wells H, Ayalew G et al. Coronavirus and
737 paramyxovirus shedding by bats in a cave and buildings in Ethiopia. EcoHealth. 2022; 19:
738 216–232.

739 25. Seltmann A, Corman VM, Rasche A, Drosten C, Á Czirják G, Bernard H, et al. Seasonal
740 fluctuations of astrovirus, but not coronavirus shedding in bats inhabiting human-
741 modified tropical forests. EcoHealth. 2017; 14: 272–284.

742 26. Pauly M, Pir JB, Loesch C, Sausy A, Snoeck CJ, Hübschen JM, Muller CP. Novel
743 alphacoronaviruses cocirculate with type 1 and severe acute respiratory system (SARS)-
744 related betacoronaviruses in synanthropic bats of Luxembourg. AEM. 2017; 83: e01326-
745 17

746 27. Petney TN, Andrews RH/ Multiparasite communities in animals and humans: frequency,
747 structure and pathogenic significance. Int. J. Parasitol. 1998; 28: 377–393.

748 28. Graham AL. Ecological rules governing helminth-microparasite coinfection. PNAS. 2008;
749 105: 566-570.

750 29. Telfer S, Lambin X, Birtles R, Beldomenico P, Burthe S, Paterson S, et al. Species
751 interactions in a parasite community drive infection risk in a wildlife population. Science.
752 2010; 330: 243–246.

753 30. Warren BH, Simberloff D, Ricklefs RE, Aguilée R, Condamine FL, Gravel D, et al. Islands as
754 model systems in ecology and evolution: prospects fifty years after MacArthur-Wilson.
755 Ecol. Lett. 2015; 18: 200–217.

756 31. Emerson BC. Evolution on oceanic islands: molecular phylogenetic approaches to
757 understanding pattern and process. Mol. Ecol. 2002; 11: 951–966.

758 32. Jean K, Burnside WR, Carlson L, Smith K, Guégan J. An equilibrium theory signature in the
759 island biogeography of human parasites and pathogens. Glob. Ecol. Biogeogr. 2016; 25:
760 107–116.

761 33. Tortosa P, Pascalis H, Guernier V, Cardinale E, Le Corre M, Goodman SM, et al.
762 Deciphering arboviral emergence within insular ecosystems. Infect. Genet. Evol. 2012; 12:
763 1333–1339.

764 34. Kier G, Kreft H, Ming Lee T, Jetz W, Ibisch PL, Nowicki C et al. A global assessment of
765 endemism and species richness across island and mainland regions. Proc. Natl. Acad. Sci.
766 2009; 106: 9322–9327.

767 35. Conenna I, Rocha R, Russo D, Cabeza M. Insular bats and research effort: A review of
768 global patterns and priorities. Mam. Rev. 2017; 47: 169–182.

769 36. Plowright RK, Becker DJ, McCallum H, Manlove KR. Sampling to elucidate the dynamics of
770 infections in reservoir hosts. Phil. Trans. R. Soc. B. 2019; 374: 20180336.

771 37. Peel AJ, Baker KS, Hayman DTS, Broder CC, Cunningham AA, Fooks AR, et al. Support for
772 viral persistence in bats from age-specific serology and models of maternal immunity. Sci.
773 Rep. 2018; 8: 3859.

774 38. Betke M, Hirsh DE, Makris NC, McCracken GF, Procopio M, Hristov NI, et al. Thermal
775 imaging reveals significantly smaller Brazilian free-tailed bat colonies than previously
776 estimated. J Mammal. 2008; 89: 18–24.

777 39. Mcfarlane D, Rentergem G, Ruina A, Lundberg J, Christenson K. Estimating colony size of
778 the Wrinkle-lipped bat, *Chaerephon plicatus* (Chiroptera: Molossidae) at Gomantong,
779 Sabah, by quantitative image analysis. Acta Chiropt. 2015; 17: 171–177.

780 40. Goodman SM, van Vuuren BJ, Ratrimomanarivo F, Probst J-M, Bowie RCK. Specific status
781 of populations in the Mascarene Islands referred to *Mormopterus acetabulosus*
782 (Chiroptera: Molossidae), with description of a new Species. J. Mammal. 2008 ; 89: 1316–
783 1327.

784 41. Cadet T. Données récentes sur l'origine, l'âge et la structure géologique de l'île de la
785 Réunion. *Académie de l'île de la réunion Bulletin 1969-1978.* 1980; 73–87.

786 42. Lagabrielle E, Rouget M, Payet K, Wistebaar N, Durieux L, Baret S et al. Identifying and
787 mapping biodiversity processes for conservation planning in islands: A case study in
788 Réunion Island (Western Indian Ocean). Biol. Conserv. 2009; 142: 1523–1535.

789 43. Dietrich M, Wilkinson DA, Benlali A, Lagadec E, Ramasindrazana B, Dellagi K, et al.
790 Leptospira and paramyxovirus infection dynamics in a bat maternity enlightens pathogen
791 maintenance in wildlife. Environ. Microbiol. 2015; 17: 4280–4289.

792 44. Aguillon S, Castex C, Duchet A, Turpin M, Le Minter G, Lebarbenchon C, et al. Landing on
793 a small tropical island: wide in-situ diversification of an urban-dwelling bat. Glob. Ecol.
794 Conserv. 2024; 53: e03030.

795 45. Joffrin L, Hoarau AOG, Lagadec E, Köster M, Ramanantsalama RV, Mavingui P et al.
796 Astrovirus in Reunion free-tailed Bat (*Mormopterus francoismoutoui*). Viruses. 2021; 13:
797 1524.

798 46. Robardet E, Borel C, Moinet M, Jouan D, Wasniewski M, Barrat J, et al. Longitudinal
799 survey of two serotine bat (*Eptesicus* serotinus) maternity colonies exposed to EBLV-1
800 (European Bat Lyssavirus type 1): Assessment of survival and serological status variations
801 using capture-recapture models. PLOS Negl. Trop. Dis. 2017; 11: e0006048.

802 47. Moreira Marrero L, Botto Nuñez G, Malta L, Delfraro A, Frabasile S. Ecological and
803 conservation significance of herpesvirus infection in neotropical bats. EcoHealth. 2021;
804 18: 123–133.

805 48. Griffiths ME, Broos A, Bergner LM, Meza DK, Suarez NM, da Silva Filipe A, et al.
806 Longitudinal deep sequencing informs vector selection and future deployment strategies
807 for transmissible vaccines. PLOS Biol. 2022; 20: e3001580.

808 49. Héré L, Probst J-M, Lequette B. Contribution à l'étude des chiroptères de l'île de La
809 Réunion. Répartition et habitats prioritaires en matière de conservation. Université de La
810 Réunion. Rapport de stage de Master. 2009.

811 50. Plowright RK, Eby P, Hudson PJ, Smith IL, Westcott D, Bryden WL et al. Ecological
812 dynamics of emerging bat virus spillover. Proc. R. Soc. B: Biol. Sci. 2015; 282: 20142124.

813 51. Serra-Cobo J, López-Roig M, Seguí M, Pilar Sánchez L, Nadal J, Borrás M, et al. Ecological
814 factors associated with European bat lyssavirus seroprevalence in Spanish bats. PLOS
815 ONE. 2013; 8: e64467.

816 52. Streicker DG, Recuenco S, Valderrama W, Gomez Benavides J, Vargas I, Pacheco V, et al.
817 Ecological and anthropogenic drivers of rabies exposure in vampire bats: implications for
818 transmission and control. Proc. Biol. Sci. 2012; 279: 3384–3392.

819 53. Laughlin AJ, Hall RJ, Taylor CM. Ecological determinants of pathogen transmission in
820 communally roosting species. Theor. Ecol. 2019; 12: 225–235.

821 54. Baker KS, Suu-Ire R, Barr J, Hayman DTS, Broder CC, Horton DL, et al. Viral antibody
822 dynamics in a chiropteran host. J. Anim. Ecol. 2014; 83: 415–428.

823 55. Epstein JH, Baker ML, Zambrana-Torrelio C, Middleton D, Barr JA, Dubovi E, et al.
824 Duration of maternal antibodies against Canine distemper virus and Hendra virus in
825 Pteropid Bats. PLOS ONE. 2013; 8: e67584.

826 56. Storm N, Jansen van Vuren P, Markotter W, Paweska JT. Antibody responses to Marburg
827 virus in Egyptian rousette bats and their role in protection against infection. Viruses.
828 2018; 10: 73.

829 57. Juman MM, Gibson L, Suu-Ire RD, Languon S, Quaye O, Fleischer G, et al. Ecological and
830 reproductive cycles drive Henipavirus seroprevalence in the African straw-coloured fruit
831 bat (*Eidolon* helvum). Ecol. Evol. 2024; 14: e70555.

832 58. Guerra-Silveira F, Abad-Franch F. Sex bias in infectious disease epidemiology: Patterns
833 and processes. PLOS ONE. 2013; 8: e62390.

834 59. Zuk M. The sicker sex. PLOS Pathog. 2009; 5: e1000267.

835 60. Erazo D, Pedersen AB, Gallagher K, Fenton A. Who acquires infection from whom?
836 Estimating herpesvirus transmission rates between wild rodent host groups. Epidemics.
837 2021; 35: 100451.

838 61. Rossetto F, Iglesias-Caballero M, Liedtke HC, Gomez-Mestre I, Berciano JM, Pérez-Suárez
839 G,et al. Mating strategy is determinant of adenovirus prevalence in European bats. PLOS
840 ONE. 2020; 15: e0226203.

841 62. Sjodin AR, Willig MR, Anthony SJ. Quantitative Delineation of Herpesviruses in Bats for
842 use in Ecological Studies. Ecology. 2019.

843 63. Ancillotto L, Russo D. Selective aggressiveness in European free-tailed bats (*Tadarida*
844 *teniotis*): influence of familiarity, age and sex. Naturwissenschaften. 2014; 101: 221–228.

845 64. Ortega J, Guerrero JA, Maldonado JE. Aggression and tolerance by dominant males of
846 Artibeus jamaicensis: strategies to maximize fitness in harem groups. J. Mammal. 2008;
847 89: 1372–1378.

848 65. Becker DJ, Bergner LM, Bentz AB, Orton RJ, Altizer S, Streicker DG. Genetic diversity,
849 infection prevalence, and possible transmission routes of Bartonella spp. in vampire bats.
850 PLOS Negl. Trop. Dis. 2018; 12: e0006786.

851 66. Foo YZ, Nakagawa S, Rhodes G, Simmons LW. The effects of sex hormones on immune
852 function: a meta-analysis. Biol. Rev. 2017; 92: 551–571.

853 67. Klein SL. Hormonal and immunological mechanisms mediating sex differences in parasite
854 infection. Parasite Immunol. 2004; 26: 247–264.

855 68. Cohen JI. Herpesvirus latency. J. Clin. Invest. 2020; 130: 3361–3369.

856 69. Gerow CM, Rapin N, Voordouw MJ, Elliot M, Misra V, Subudhi S. Arousal from
857 hibernation and reactivation of *Eptesicus fuscus* gammaherpesvirus (*Ef* HV) in big brown
858 bats. Transbound Emerg. Dis. 2018; 66: 1054–1062.

859 70. Griffiths ME, Meza DK, Haydon DT, Streicker DG. Inferring the disruption of rabies
860 circulation in vampire bat populations using a betaherpesvirus-vectored transmissible
861 vaccine. Proc. Natl. Ac. Sci. 2023; 120: e2216667120.

862 71. Aguillon S, Turpin M, Le Minter G, Lebarbenchon C, Hoarau AOG, Mavingui P, Dietrich M.
863 Bat things come in threes: within-host dynamics of herpesvirus triple infection in bats.
864 bioRxiv 2025.02.05.636680.

865 72. Mortlock M, Geldenhuys M, Dietrich M, Epstein JH, Weyer J, Paweska JT, Markotter W.
866 Seasonal shedding patterns of diverse henipavirus-related paramyxoviruses in Egyptian
867 rousette bats. Sci. Rep. 2021; 11 : 24262.

868 73. Almeida DS, Nogueira Paz L, Santos de Oliveira D, Nascimento Silva D, Ristow P, Hamond
869 C, et al. Investigation of chronic infection by Leptospira spp. in asymptomatic sheep
870 slaughtered in slaughterhouse. PLOS ONE. 2019; 14: e0217391.

871 74. Cordonin C, Turpin M, Bringart M, Bascands J-L, Flores O, Dellagi K, et al. Pathogenic
872 Leptospira and their animal reservoirs: testing host specificity through experimental
873 infection. Sci. Rep. 2020; 10: 7239.

874 75. Ratet G, Veyrier FJ, Fanton d'Andon M, Kammerscheit X, Nicola M-A, Picardeau M, et al.
875 Live imaging of bioluminescent *Leptospira interrogans* in mice reveals renal colonization
876 as a stealth escape from the blood defenses and antibiotics. PLOS Negl. Trop. Dis. 2014;
877 8: e3359.

878 76. Glennon EE, Becker DJ, Peel AJ, Garnier R, Suu-Ire RD, Gibson L, et al. What is stirring in
879 the reservoir? Modelling mechanisms of henipavirus circulation in fruit bat hosts. Phil.
880 Trans. R. Soc. B. 2019; 374: 20190021.

881 77. Gibson L, Puig Ribas M, Kemp J, Restif O, Suu-Ire RD, Wood JLN, et al. Persistence of
882 multiple paramyxoviruses in a closed captive colony of fruit bats (*Eidolon helvum*).
883 Viruses. 2021; 13: 1659.

884 78. Peel AJ, Baker KS, Crameri G, Barr JA, Hayman DTS, Wright E, et al. Henipavirus
885 neutralising antibodies in an isolated island population of African fruit bats. PLOS ONE.
886 2012; 7: e30346.

887 79. Rahman SA, Hassan SS, Olival KJ, Mohamed M, Chang L-Y, Hassan L, et al.
888 Characterization of Nipah virus from naturally infected *Pteropus vampyrus* Bats,
889 Malaysia. Emerg. Infect. Dis. 2010; 16: 1990–1993.

890 80. Sohayati AR, Hassan L, Sharifah SH, Lazarus K, Zaini CM, Epstein JH, et al. Evidence for
891 Nipah virus recrudescence and serological patterns of captive *Pteropus vampyrus*.
892 Epidemiol. Infect. 2011; 139: 1570–1579.

893 81. Plowright RK, Foley P, Field HE, Dobson AP, Foley JE, Eby P, et al. Urban habituation,
894 ecological connectivity and epidemic dampening: the emergence of Hendra virus from
895 flying foxes (Pteropus spp.). Proc. Biol. Sci. 2011; 278: 3703–3712.

896 82. Gentles AD, Guth S, Rozins S, Brook CE. A review of mechanistic models of viral dynamics
897 in bat reservoirs for zoonotic disease. Pathog. Glob. Health. 2020; 114: 407-425.

898 83. Becker DJ, Ketterson ED, Hall RJ. Reactivation of latent infections with migration shapes
899 population-level disease dynamics. Proc. R. Soc. B. 2020; 287: 20201829.

900 84. Grinde B. Herpesviruses: latency and reactivation – viral strategies and host response. J.
901 Oral. Microbiol. 2013; 5: 10.3402/jom.v5i0.22766.

902 85. Negrey JD, Thompson ME, Dunn CD, Otali E, Wrangham RW, Mitani JC, et al. Female
903 reproduction and viral infection in a long-lived mammal. J. Anim. Ecol. 2022; 91: 1999–
904 2009.

905 86. Butte NF, Wong WW, Treuth MS, Ellis KJ, O'Brian Smith E. Energy requirements during
906 pregnancy based on total energy expenditure and energy deposition. Am. J. Clin. Nutr.
907 2004; 79: 1078–1087.

908 87. Speakman JR. The physiological costs of reproduction in small mammals. Philos. Trans. R.
909 Soc. Lond. B Biol. Sci. 2008; 363: 375–398.

910 88. Plowright RK, Field HE, Smith C, Divljan A, Palmer C, Tabor G, et al. Reproduction and
911 nutritional stress are risk factors for Hendra virus infection in little red flying foxes
912 (*Pteropus scapulatus*). Proc. Biol. Sci. 2008; 275: 861–869.

913 89. Encarnação JA, Dietz M, Kierdorf U. Reproductive condition and activity pattern of male
914 Daubenton's bats (*Myotis daubentonii*) in the summer habitat. Mamm. Biol. 2004; 69:
915 163–172.

916 90. Martin L, Bernard RT. Endocrine regulation of reproduction in bats: the role of circulating
917 gonadal hormones. In *Reproductive Biology of Bats*, (Elsevier) 2000; pp. 27–64.

918 91. Ruoss S, Becker NI, Otto MS, Czirják GA, Encarnação JA. Effect of sex and reproductive
919 status on the immunity of the temperate bat *Myotis daubentonii*. Mamm. Biol. 2019; 94:
920 120–126.

921 92. Dietrich M, Kearney T, Seamark ECJ, Paweska JT, Markotter W. Synchronized shift of oral,
922 faecal and urinary microbiotas in bats and natural infection dynamics during seasonal
923 reproduction. R. Soc. Open Sci. 2018; 5: 180041.

924 93. Drexler JF, Corman VM, Wegner T, Tateno AF, Zerbinati RM, Gloza-Rausch F et al.
925 Amplification of Emerging Viruses in a Bat Colony. Emerg. Infect. Dis. 2011; 17: 449–456.

926 94. Mourad M, Gershon M, Mehta SK, Crucian BE, Hubbard N, Zhang J, et al. Silent
927 Reactivation of Varicella zoster virus in pregnancy: Implications for maintenance of
928 immunity to varicella. Viruses. 2022; 14: 1438.

929 95. Alizon S. Co-infection and super-infection models in evolutionary epidemiology. Interface
930 Focus. 2013; 3: 20130031.

931 96. Habig B, Chowdhury S, Monfort SL, Brown JL, Swedell L, Foersterh S. Predictors of
932 helminth parasite infection in female chacma baboons (*Papio ursinus*). Int. J. Parasitol.
933 Parasites Wildl. 2021; 14: 308–320.

934 97. Eby P, Peel AJ, Hoegh A, Madden W, Giles JR, Hudson PJ, et al. Pathogen spillover driven
935 by rapid changes in bat ecology. Nature. 2022; 613: 340–344.

936 98. Markotter W, Vries LD, Paweska J. Wing tattoos: A cost-effective and long-lasting method
937 for marking bats. Acta Chiropt. 2023; 25: 193–202.

938 99. Lebarbenchon C, Ramasindrazana B, Joffrin L, Bos S, Lagadec E, Le Minter G, et al.
939 Astroviruses in bats, Madagascar. Emerg. microbes & infect. 2017; 6: 1–3.

940 100. Smythe LD, Smith IL, Smith GA, Dohnt MF, Symonds ML, Barnett LJ et al. A quantitative
941 PCR (TaqMan) assay for pathogenic Leptospira spp. BMC Infect. Dis. 2002; 2: 13.

942 101. Tong S, Chern S-WW, Li Y, Pallansch MA, Anderson LJ. Sensitive and broadly reactive
943 reverse transcription-PCR assays to detect novel paramyxoviruses. J. Clin. Microbiol.
944 2008; 46: 2652–2658.

945 102. VanDevanter DR, Warrener P, Bennett L, Schultz ER, Coulter S, Garber RL, et al. Detection
946 and analysis of diverse herpesviral species by consensus primer PCR. J. Clin. Microbiol.
947 1996; 34: 1666–1671.

103. Bjørnstad, ON. *Ncf: Spatial nonparametric covariance functions. R package version 1.1-3. 2009.*

104. Paez A. Grey literature: An important resource in systematic reviews. J. Evid. Based. Med. 2017; 10: 233-240.

105. Holmes EE, Ward EJ, Wills K. MARSS: Multivariate autoregressive state-space models for analyzing time-series data. The R Journal. 2012: 11-19.

106. Zuur AF, Tuck ID, Bailey N. Dynamic factor analysis to estimate common trends in fisheries time series. Cam. J. Fish. Aquat. Sci. 2003; 60: 542-552.

107. Wood SN, *Generalized additive models: An introduction with R* (CRC press). 2017.

108. Bonenfant C, Gaillard J-M, Dray S, Loison A, Royer M, Chessel D. Testing sexual segregation and aggregation: old ways are best. Ecology. 2007; 88: 3202–3208.

109. Streicker DG, Fallas González SL, Luconi G, Barrientos RG, Leon B. Phylodynamics reveals extinction–recolonization dynamics underpin apparently endemic vampire bat rabies in Costa Rica. Proc. R. Soc. B. 2019; 286: 20191527.

110. RStudio Team*. RStudio: integrated development for R*. *Rstudio Team, PBC, Boston, MA.* 2020.

111. QGIS Development Team, QGIS Geographic Information System. Open Source Geospatial Foundation Project. (2022). Available at: http://qgis.osgeo.org [Accessed 27 July 2023].

Figures

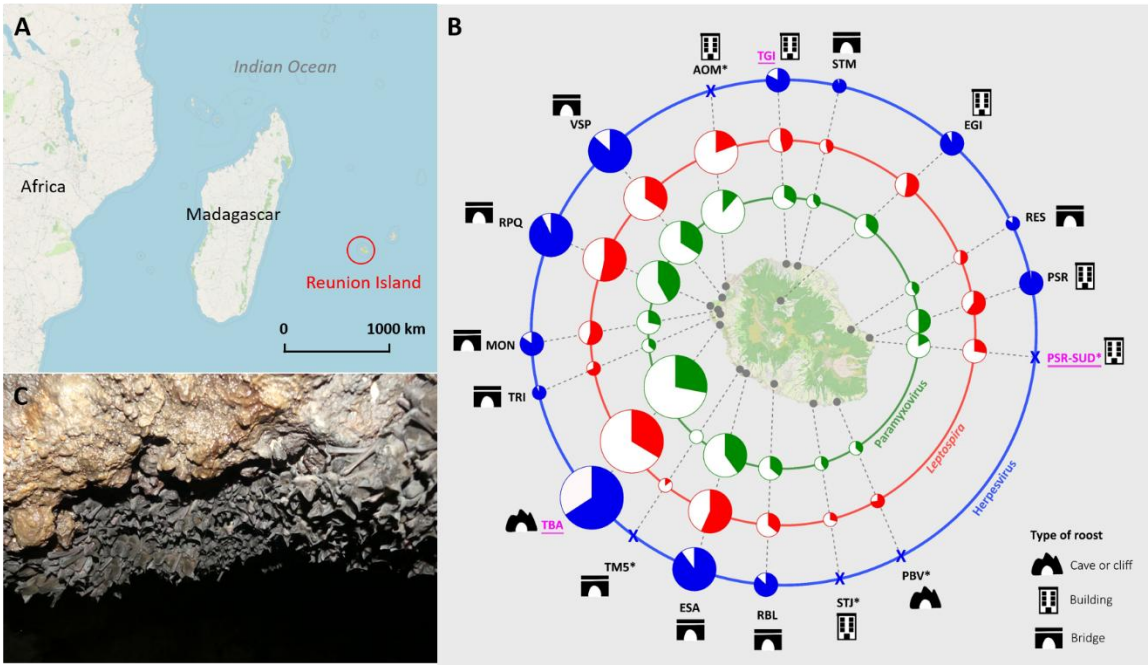

Fig 1. Widespread triple shedding in *Mormopterus francoismoutoui.* (A) Location of Reunion Island and (B) the studied roosts. (C) A picture of juvenile bats aggregated in the maternity roost (TBA). In (B) studied roosts are represented by grey circles on Reunion Island map and prevalence (color section of pie charts) is represented for paramyxoviruses (in green), *Leptospira* bacteria (in red) and herpesviruses (in blue). A cross denotes the absence of prevalence data (no tested samples). Pie diameter corresponds to four categories of roost size: small < 500 individuals, medium: 500-2000 individuals, high: 2000-6000 individuals, and exceptional > 100,000 individuals. Accurate roost size estimation was not being performed for EGI and PSR roosts, but they are represented as medium roosts because several hundred/thousands are expected. Maternity roosts are underlined in pink. Roosts that were monitored only once are depicted by an asterisk. Maps were created using Qgis [111] with a background of OpenStreetMap France under License CC- BY- SA 2.0. This figure was inspired by Streicker et al. 2012 [52].

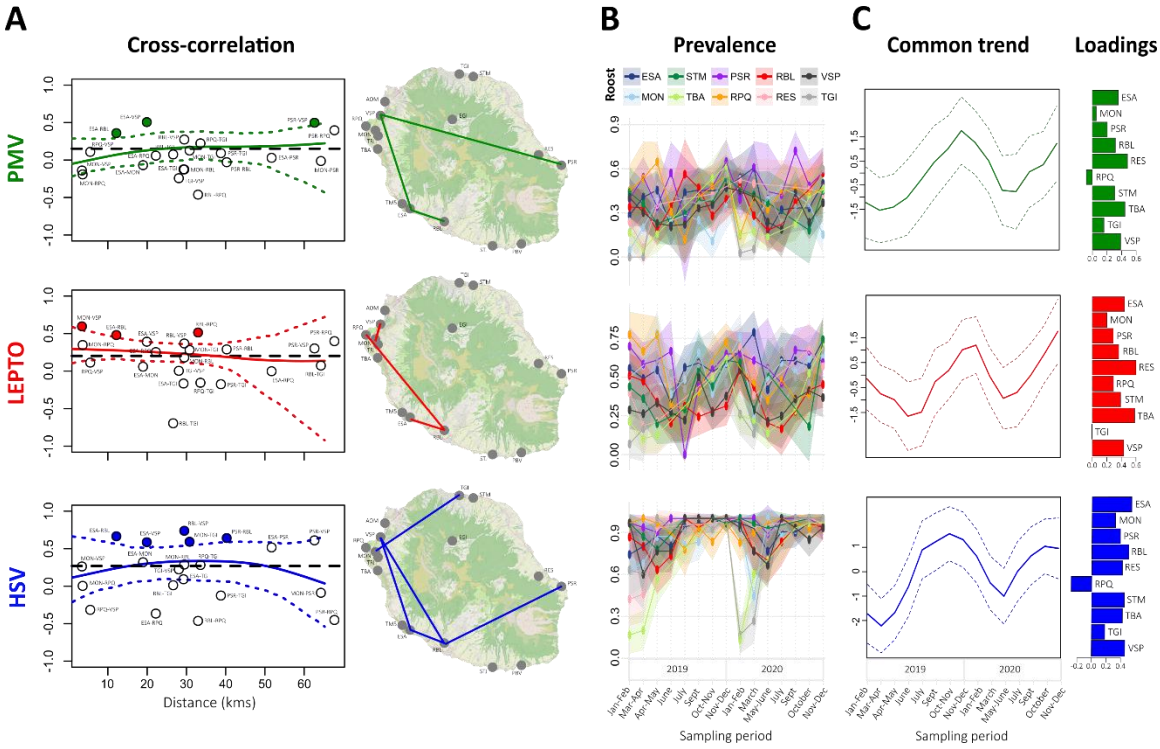

Fig 2. Synchrony of prevalence across roosts for paramyxoviruses (PMV), *Leptospira* bacteria (LEPTO) and herpesviruses (HSV) in *M. francoismoutoui*. (A) Pairwise Pearson's correlation coefficients are depicted in relation to geographical distance between roosts. Coefficients were not calculated for TBA, RES, and STM roosts because of missing data during winter (these roosts were empty at this time). The spline correlogram (thick colored line) and 95% confidence interval (dotted colored lines) are shown. The mean estimated synchrony is represented by the black dotted line. Positive correlation coefficients that exceed the spline's confidence interval are highlighted with colored circles and are represented on the map by connecting lines between roosts. (B) Roost-specific raw prevalence across time (thick line) and 95% confidence interval (colored band). (C) Estimated common prevalence trend (thick line) across time and confidence interval (dotted lines). Loadings describing the relationships between roosts and the common trend are shown on the right. Three-letter code refers to roost name as in Table 1. Maps were created using Qgis [111] with a background of OpenStreetMap France under License CC- BY- SA 2.0.

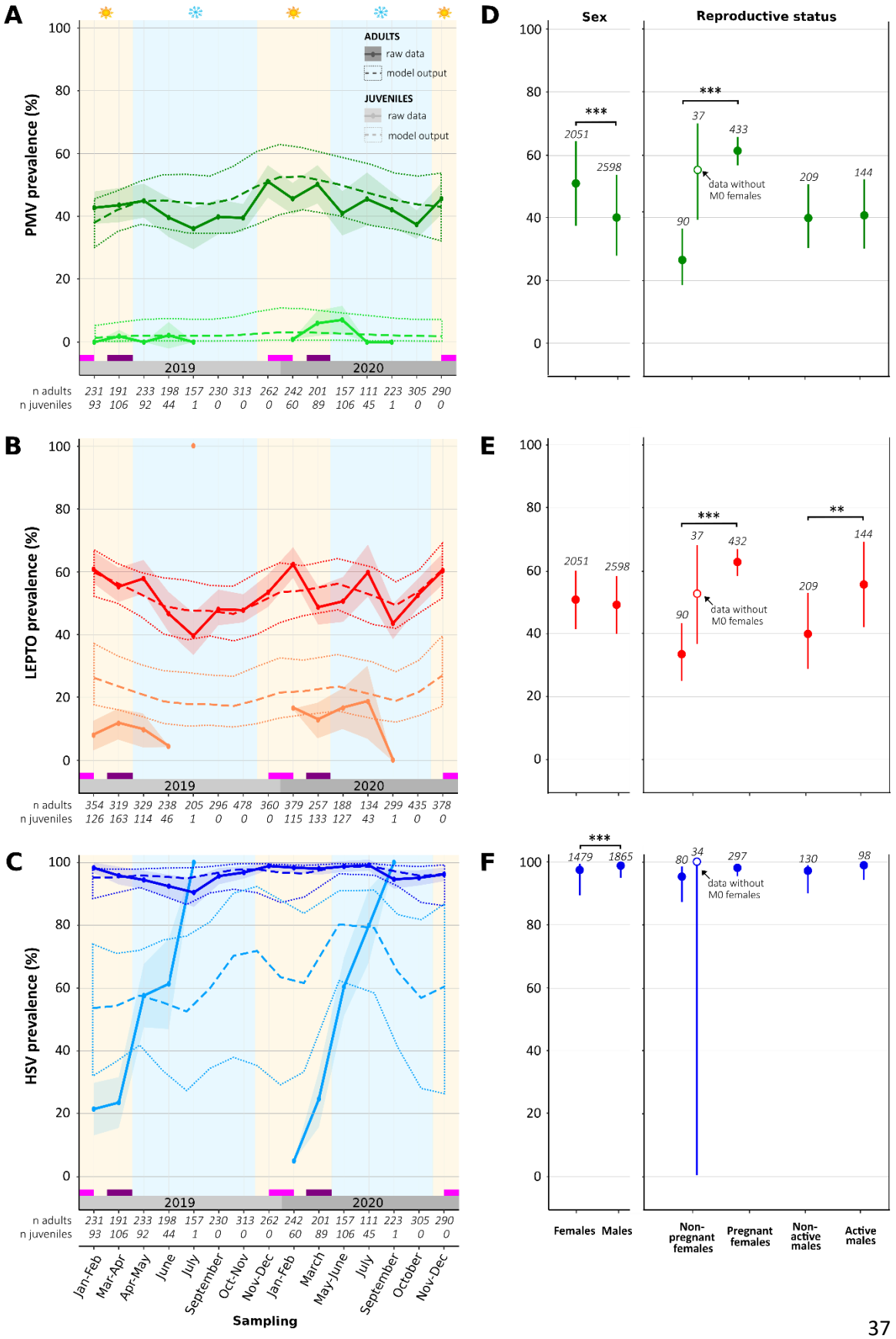
A
PMV prevalence (%)
ADULTS
raw data
model output
JUVENILES
raw data
model output
2019
2020
n adults 231 191 233 198 157 230 313 262 242 201 157 111 223 305 290
n juveniles 93 106 92 44 1 0 0 0 60 89 106 45 1 0 0
B
LEPTO prevalence (%)
2019
2020
n adults 354 319 329 238 205 296 478 360 379 257 188 134 299 435 378
n juveniles 126 163 114 46 1 0 0 0 115 133 127 43 1 0 0
C
HSV prevalence (%)
2019
2020
n adults 231 191 233 198 157 230 313 262 242 201 157 111 223 305 290
n juveniles 93 106 92 44 1 0 0 0 60 89 106 45 1 0 0
Jan-Feb
Mar-Apr
Apr-May
June
July
September
Oct-Nov
Nov-Dec
Jan-Feb
March
May-June
July
September
October
Nov-Dec
Sampling
D
Sex
Reproductive status
***
2051
2598
***
37
433
90
209
144
data without M0 females
E
2051
2598
***
37
432
90
data without M0 females
**
209
144
F
***
1479
1865
80
34
297
130
98
data without M0 females
Females
Males
Non-pregnant females
Pregnant females
Non-active males
Active males

1005

1006 **Fig 3. Age and reproduction periods drive paramyxovirus (PMV), *Leptospira* bacteria**
1007 **(LEPTO) and herpesvirus (HSV) shedding dynamics in *M. francoismoutoui.*** (A-C) The
1008 observed prevalence (raw data) is represented by solid lines, with by 95% confidence
1009 intervals shown as shaded areas. Predicted prevalence and binomial sampling errors
1010 (model output) are depicted by dotted lines. Pink and purple blocks at the bottom
1011 represent the parturition and the mating periods, respectively. Austral summer and
1012 winter are indicated in yellow and blue, respectively. (D-F) Predicted prevalence (and
1013 binomial sampling errors) in adults according to their sex and reproductive status (active
1014 or not). Significant effects of GAMs (S1 and S3 Tables) are indicated: *** $P < 0.001$ and **
1015 $P < 0.01$.

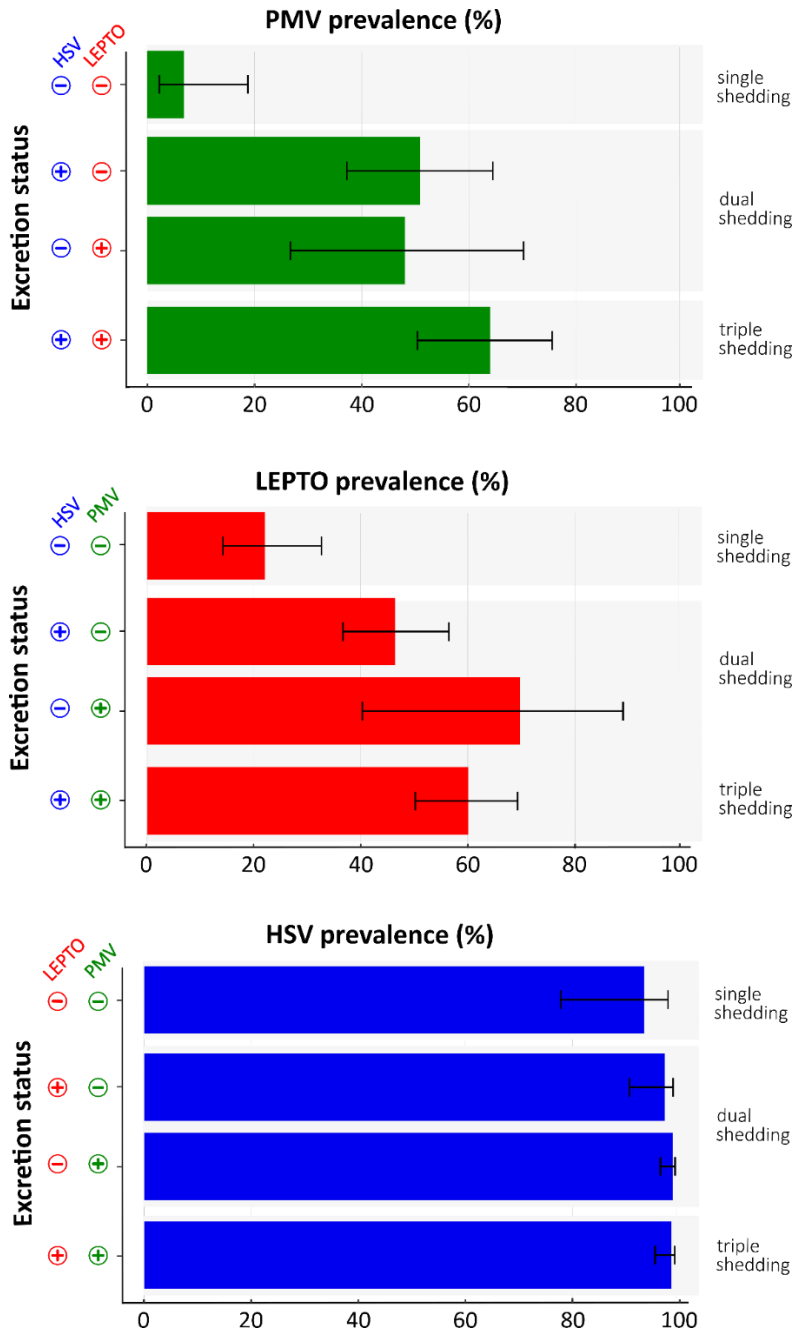

Fig 4. Shedding probability increases with dual and triple infections in *M. francoismoutoui*. Prevalence estimates were derived from the predicted probabilities generated by GAMs M1-M3. Shedding status is coded with 0 for non-shedding bats and 1 for bats shedding infectious agent(s). Black bars indicate the 95% confidence intervals.

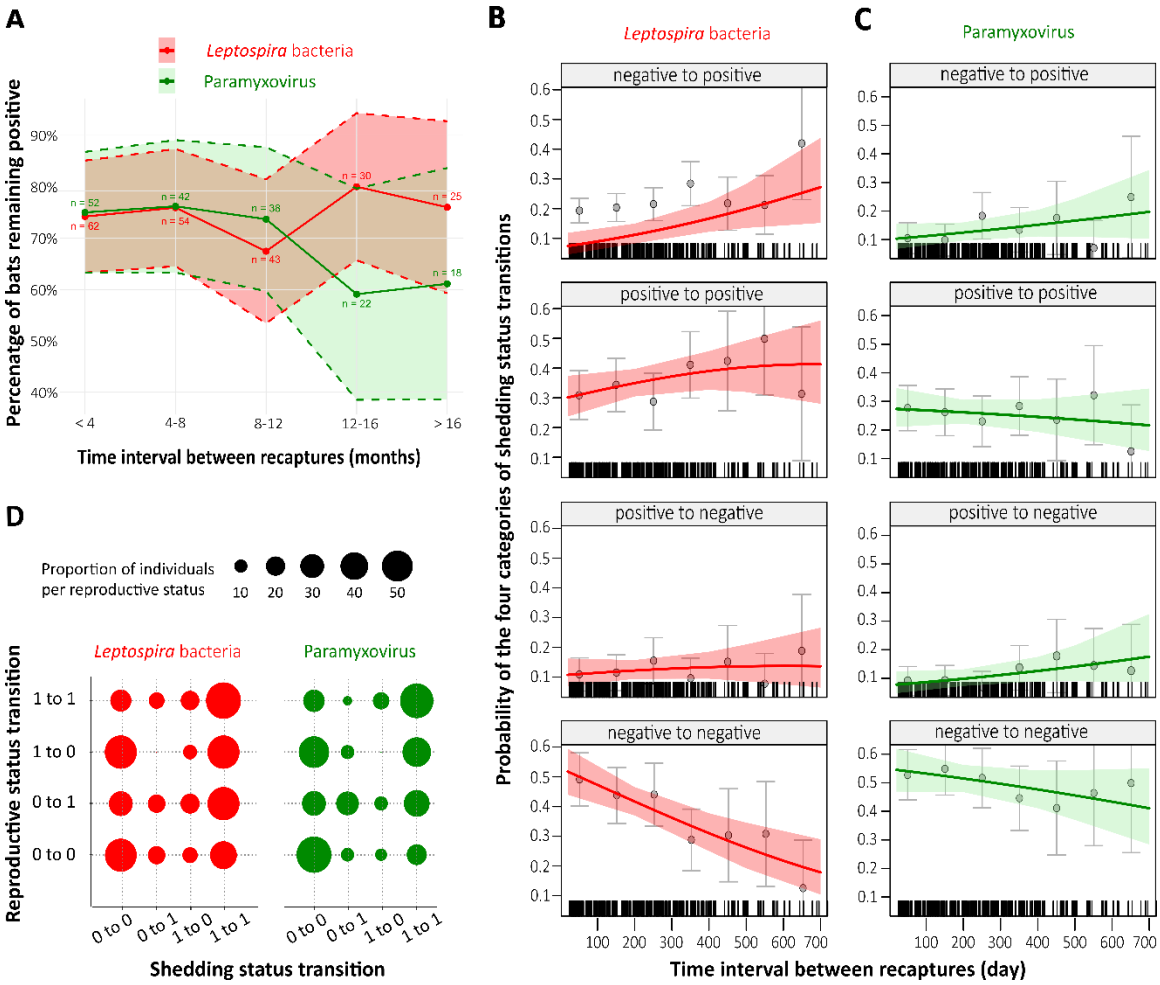

Fig 5. Shedding histories in recaptured *M. francoismoutoui* bats. (A) Percentage of bats remaining *Leptospira* and paramyxovirus positive through time. (B-C) Probability of the four categories of shedding status transitions over time, for (B) *Leptospira* and (C) paramyxovirus. Predicted values (output of the multinomial models) and 95% confidence intervals are depicted with colored lines and shaded areas. Raw proportions (and 95% CI) are represented with grey circles and bars for each interval of 100 days. (D) Proportion of recaptured bats according to changes in shedding status and reproductive status. Shedding status is coded with 0 for non-shedding and 1 for shedding bats. Reproductive status is coded with 0 for non-active and 1 for active bats.